

1 **Genome-wide characterization of the Fur regulatory network reveals a link**
2 **between catechol degradation and bacillibactin metabolism in *Bacillus subtilis***

3
4
5 **running title: Catechol degradation during bacillibactin metabolism**

6 Hualiang Pi^a and John D. Helmann^{a#}

7
8
9
10
11 Author Information

12 ^a*Department of Microbiology, Cornell University, Ithaca, NY 14853-8101, USA*

13 #For correspondence: E-mail: jdh9@cornell.edu, Phone: 607-255-6570

14
15
16
17 Keywords: Fur regulon, ChIP-seq, catechol degradation, bacillibactin metabolism

18

19 **Abstract.** The ferric uptake regulator (Fur) is the global iron biosensor in many bacteria. Fur
20 functions as an iron-activated transcriptional repressor for most of its regulated genes. There
21 are a few examples where holo-Fur activates transcription, either directly or indirectly. Recent
22 studies suggest that apo-Fur might also act as a positive regulator and, besides iron metabolism,
23 the Fur regulon might encompass other biological processes such as DNA synthesis, energy
24 metabolism, and biofilm formation. Here, we obtained a genomic view of the Fur regulatory
25 network in *Bacillus subtilis* using ChIP-seq. Besides the known Fur target sites, 70 putative DNA
26 binding sites were identified, and the vast majority had higher occupancy under iron sufficient
27 conditions. Among the new sites detected, a Fur binding site in the promoter region of the
28 *catDE* operon is of particular interest. This operon, encoding catechol 2,3-dioxygenase, is critical
29 for catechol degradation and is under negative regulation by CatR and YodB. These three
30 repressors function cooperatively to regulate the transcription of *catDE*, with Fur functioning as
31 a sensor of iron-limitation and CatR as the major sensor of catechol stress. Genetic analysis
32 suggests that CatDE is involved in metabolism of the catecholate siderophore bacillibactin,
33 particularly when bacillibactin is constitutively produced and accumulates intracellularly,
34 potentially generating endogenous toxic catechol derivatives. This study documents a role for
35 catechol degradation in bacillibactin metabolism, and provides evidence that catechol 2,3-
36 dioxygenase can detoxify endogenously produced catechol substrates in addition to its more
37 widely studied role in biodegradation of environmental aromatic compounds and pollutants.

38

39 **Importance.** Many bacteria synthesize high affinity iron chelators (siderophores). Siderophore-
40 mediated iron acquisition is an efficient and widely utilized strategy for bacteria to meet their

41 cellur iron requirements. One prominent class of siderophores uses catecholate groups to
42 chelate iron. *B. subtilis* bacillibactin, structurally similar to enterobactin (made by enteric
43 bacteria), is a triscatecholate siderophore that is hydrolyzed to monomeric units after import to
44 release iron. However, the ultimate fate of these catechol compounds and their potential
45 toxicity have not been defined previously. Here, we performed genome-wide identification of
46 Fur binding sites *in vivo* and uncovered a connection between catechol degradation and
47 bacillibactin metabolism in *B. subtilis*. Beside its role in detoxification of environmental
48 catechols, the catechol 2,3-dioxygenase encoded by *catDE* also protects cells from intoxication
49 by endogenous bacillibactin-derived catechol metabolites under iron-limited conditions. These
50 findings shed light on the degradation pathway and precursor recycling of the catecholate
51 siderophores.

52

53 **Introduction**

54 Iron is an essential micronutrient for most bacteria. It is required for many biological
55 processes but can be toxic when present in excess. Various iron-mediated stress systems
56 respond to changes in environmental iron availability (1, 2). Iron limitation induces acquisition
57 systems to scavenge iron from the surroundings and activates systems to mobilize and prioritize
58 iron utilization (3). Conversely, iron excess induces storage and efflux systems to maintain non-
59 toxic levels of intracellular free labile iron (4, 5). These responses must be carefully coordinated
60 by iron responsive regulators to ensure effective iron balance within the cell. The ferric uptake
61 regulator (Fur) is the key regulator of iron homeostasis in many bacteria (6, 7). Fur monitors

62 intracellular iron levels and regulates transcription of systems for iron uptake, utilization,
63 storage, and efflux (7-9).

64 The Fur regulon has been characterized in many bacteria. In *B. subtilis*, the Fur regulon
65 consists of an estimated 29 operons, many of which are involved in iron acquisition. These
66 encode the biosynthesis machinery for the endogenous siderophore (bacillibactin, BB), and
67 uptake systems for elemental iron, ferric citrate, BB, and various xenosiderophores that are
68 secreted by other microbes (9). In general, Fur functions as an iron-activated transcriptional
69 repressor for most of its regulon. Under iron replete conditions, Fur binds to its cofactor Fe^{2+}
70 and the resulting holo-Fur binds to its target sites and represses transcription of its target genes;
71 when iron is limited Fur loses its cofactor and apo-Fur dissociates from DNA leading to
72 derepression of its regulon. Recent results reveal that the Fur regulon is derepressed in three
73 sequential waves (3). As cells transition from iron sufficiency to deficiency, *Bacillus* cells (i)
74 increase their capacity for import of common forms of chelated iron that are already in their
75 environment such as elemental iron and ferric citrate, (ii) invest their energy to synthesize their
76 own siderophore BB and produce high affinity siderophore-mediated import systems to
77 scavenge iron, and (iii) activate a small RNA FsrA and its partner proteins to prioritize iron
78 utilization (3).

79 In addition to its regulatory role as a transcriptional repressor, holo-Fur can also activate
80 gene expression, either directly or indirectly (5, 10, 11). For instance, in *Escherichia coli* Fur
81 positively regulates expression of the iron storage gene *ftnA* by competing against the H-NS
82 repressor when iron levels are elevated (5), and *Listeria monocytogenes* Fur activates the
83 ferrous iron efflux transporter FrvA to protect cells from iron intoxication (10). Recent studies

84 suggested that apo-Fur may also act as a positive regulator (12) and, besides iron metabolism,
85 the Fur regulon may expand into other biological processes such as DNA synthesis, energy
86 metabolism, and biofilm formation (12-15). These findings motivated us to obtain a genomic
87 view of the Fur regulatory network in response to iron availability in *B. subtilis*. Besides the
88 known Fur target sites, 70 putative DNA binding sites were identified using chromatin
89 immunoprecipitation coupled with high-throughput sequencing (ChIP-seq). Our attention was
90 drawn to the binding site located in the promoter region of the *catDE* operon. This operon
91 encodes a mononuclear iron enzyme, catechol 2,3-dioxygenase, which is critical for catechol
92 degradation (16).

93 *B. subtilis* is a soil microbe. In its natural habitat, *B. subtilis* is exposed to many toxic
94 aromatic compounds that are released from decaying plants, fungi, animals, and industrial
95 wastes (17-19). Aromatic compounds are one of the most prevalent pollutants in the
96 environment and the majority of them are oxidized to catechols before the benzene rings are
97 cleaved (20). Catechols are persistent in the environment and can undergo a wide range of
98 chemical reactions outside or within the cell: (i) complex formation with heavy metals, (ii) redox
99 cycling, and (iii) production of reactive oxygen species (ROS) by reaction with metal ions and
100 oxygen. These processes can damage DNA and protein and disrupt membrane potential (21).

101 Catechol dioxygenases have been widely studied for their initiating role in
102 biodegradation of catechols, which are themselves common intermediates in the degradation
103 of a wide variety of aromatic compounds (19). Our observation of a Fur-binding site preceding
104 the *catDE* operon led us to hypothesize that, in addition to the external catechol stress, *B.*
105 *subtilis* may encounter threats from the endogenous catechol compounds. In response to iron

106 limitation, *B. subtilis* synthesizes the catechol-based siderophore BB and expresses siderophore-
107 mediated uptake systems to overcome iron deficiency. BB, structurally similar to enterobactin
108 primary found in Gram-negative bacteria (22), is synthesized through a non-ribosomal peptide
109 synthetase (NRPS) assembly system (DhbACEBF) (23). BB is secreted by a major facilitator
110 superfamily transporter YmfD (24), which is under regulation of the transcriptional activator
111 Mta (24), a MerR family regulator of multidrug-efflux transporter system. BB chelates ferric iron
112 with extremely high affinity (a pFe of $\sim 10^{-33}$ M under biological conditions; (7)) and the
113 resultant ferric-BB complex is then imported by the FeuABC-YusV system (25). Ferric-BB is
114 subsequently hydrolyzed by the BesA esterase to release iron, which yield three BB-monomers
115 (2,3-dihydroxybenzoate-glycine-threonine) (25). It is unknown whether the BB monomer is
116 further processed, but this and derived catechol-containing compounds are potentially toxic
117 and could affect cell fitness.

118 In this study, we demonstrate that holo-Fur functions as a repressor and works
119 cooperatively with two other regulators, CatR and YodB, in regulating transcription of the *catDE*
120 operon. This operon is induced upon catechol stress or iron limitation, and strongly induced
121 when both conditions are present. Furthermore, accumulation of endogenous BB-derived
122 catechol compounds triggers cell lysis and CatDE is required to alleviate the toxicity. These
123 findings suggest that CatDE is involved in metabolism of the triscatecholate siderophore BB and
124 reveal a link between catechol degradation and bacillibactin metabolism in *B. subtilis*.

125

126 **Results and discussion**

127 **Genome-wide identification of Fur-binding sites by ChIP-seq**

128 A recent study suggested that under anaerobic conditions *B. subtilis* Fur might regulate
129 genes beyond its previously defined regulon (15). Moreover, our previous genome-wide studies
130 of Fur regulation were focused on those genes (as monitored by microarray analysis) that were
131 derepressed in both a *fur* mutant and in response to iron depletion. Since Fur might also act to
132 activate gene expression, and some targets might not have been represented in the microarray
133 (which was focused on annotated ORFs), we here chose to take an unbiased view towards
134 defining those sites bound to Fur *in vivo* under both iron replete and iron deficient conditions
135 using ChIP-seq. To modulate intracellular iron levels, we employed a high-affinity Fe²⁺ exporter
136 FrvA from *L. monocytogenes* to impose iron starvation, as described previously (3, 10). *Bacillus*
137 wild-type cells (with C-terminal FLAG-tagged Fur at its native locus and an IPTG-inducible
138 ectopic copy of *frvA* integrated at *amyE* locus) were harvested at 0 and 30 min after IPTG
139 induction to study Fur-dependent regulation under iron sufficient and deficient conditions,
140 respectively (see details in “Materials and Methods”).

141

142 **Fur-dependent binding under iron deficient conditions**

143 ChIP-seq analysis identified 89 and 27 reproducible Fur-binding sites (signal to noise ratio,
144 S/N ≥ 1.5) under iron sufficient and deficient conditions, respectively (Fig. 1 and Table S3-S4).
145 Most of the binding sites (22 out of 27) occupied under iron deficient conditions overlap with
146 those under iron sufficient conditions, so the total number of binding sites are 94 (Fig. 1B).

147 These sites may represent sites bound by holo-Fur that are of particularly high affinity and slow
148 dissociation rate, or possibly sites that can be occupied *in vivo* by apo-Fur.

149 Five ChIP peaks are specific to Fur under iron deficient conditions, and could represent
150 authentic apo-Fur specific sites (Fig. S1 and Table S4). One of these sites is located in the
151 promoter of the *S477-ykoP* operon (Table S3), which encodes a possible regulatory RNA *S477*
152 and a protein YkoP with unknown function. This operon has been implicated to be under
153 negative regulation of multiple regulators including Fur (9), ResD (15), NsrR(15), and Kre (26).
154 However, a statistically significant ChIP-peak (P-value ≥ 0.05) was only detected in one of the
155 biological replicates (Table S3), indicating that the regulatory role of Fur at this site is uncertain.
156 Four other apo-Fur specific sites are located in intragenic regions and Fur occupancy at these
157 sites is fairly low (Fig. S1 and Table S4). The physiological significance of Fur-binding at these
158 sites is unclear. However, the ChIP peak located inside *ylpC* (also known as *fapR*) is very close to
159 5'-end of the gene (Fig. S1D). FapR functions as a global regulator of fatty acid biosynthesis and
160 is well conserved in Gram-positive bacteria (27). The *fapR* gene is under dual regulation:
161 negative regulation by FapR itself (28) and positive regulation by the quorum sensing regulator
162 ComA (29). Interestingly, transcriptome data show that expression of *fapR* is ~4-fold
163 upregulated in a *fur* null mutant compared to WT (9), suggesting that *fapR* might be under
164 negative regulation of Fur under iron deficient conditions. Overall, our results suggest that apo-
165 Fur has a limited role, if any, in gene regulation in *B. subtilis*. However, the connection between
166 fatty acid biosynthesis and iron homeostasis deserves further investigation.

167

168 **Known Fur target sites identified by CHIP-seq**

169 Most of the previously defined Fur target sites (24 out of 27) were detected *in vivo* by
170 CHIP-seq analysis (Fig. 1 and Table S3), which validated the modified method of CHIP-seq in *B.*
171 *subtilis* (see details in “Materials and Methods”) and further confirmed the Fur binding sites
172 characterized by *in vitro* DNase 1 footprinting and transcriptome analysis (9). However, Fur
173 occupancy at the promoter sites of *pfeT*, *yfkM*, and *ydhU/2-ydhU/1* was undetectable. The gene
174 *pfeT* encodes a Fe²⁺-efflux transporter and its expression is activated by Fur only under excess
175 iron conditions (30), which is likely why we were unable to detect Fur binding at this site under
176 the conditions tested. The gene *yfkM* encodes a general stress protein that is under regulation
177 of SigB, and *ydhU2* and *ydhU/1* are two inactive pseudogenes. The prior study only detected
178 very weak Fur binding at the promoter sites of *yfkM* and *ydhU/2-ydhU/1* *in vitro* and the Fur
179 box identified at these two sites are only 10 out of 15 bases matching to the minimal 7-1-7
180 consensus sequence (9, 31). These results, together with the lack of measurable Fur occupancy
181 *in vivo*, suggest that Fur may not play a significant role in regulation of these genes.

182

183 **CHIP peaks located in intragenic region**

184 Many of the putative Fur binding sites identified by CHIP-seq (29 out of 70 sites) are
185 located in intragenic regions (Table S4). Expression of most of these genes are not regulated by
186 Fur (comparing mRNA levels between a *fur* mutant and WT) as monitored by microarray
187 analysis (9) and qPCR (Table S4 and Table S5), indicating an apparent lack of physiological
188 relevance for these sites. We then evaluated the possible involvement of some putative targets

189 in iron homeostasis, either iron intoxication or limitation. Among the five targets tested (the
190 ones associated with high Fur occupancy i.e. *ppsB*, *gidA*, *tufA*, *ybaC* and *yycE*), none of them
191 showed sensitivity to high iron; only the *gidA* null mutant showed modest sensitivity to
192 dipyridyl compared to WT. The gene *gidA* encodes a tRNA uridine 5-
193 carboxymethylaminomethyl modification enzyme and its role in iron homeostasis is currently
194 under further investigation.

195 Another notable candidate for a functional intragenic Fur-binding site resides within
196 *ppsB*, the second gene in a long operon encoding a non-ribosomal peptide synthetase (NRPS)
197 that synthesizes the antibacterial compound plipastatin (a lipopeptide closely related to
198 fengycins) (32). This peak has the highest Fur occupancy among all the newly identified sites
199 (Table S4). A promoter and two transcription start sites in opposite directions were assigned
200 overlapping this ChIP peak (33), suggesting that transcription initiates internally to *ppsB*. In
201 addition, a putative Fur box was identified within this peak area (11 out of 15 bases matching to
202 the consensus sequence) (Table S5). The transcriptome data showed that expression of *ppsB* is
203 ~3-fold downregulated in a *fur* null mutant compared to WT, although this result was not
204 confirmed by qPCR (Table S5). The *ppsB* null mutant showed no significant sensitivity to either
205 iron intoxication or limitation compared to WT (Table S5). However, numerous studies
206 document an important stimulatory role for iron in lipopeptide production in *Bacilli* (34, 35),
207 and lipopeptides can chelate metal ions (36) and likely iron. Together, these results lead us to
208 speculate that transcripts encoded within *ppsB* may be regulated by Fur, and perhaps function
209 to coordinate plipastin synthesis with iron status.

210

211 **ChIP peaks located in regulatory regions**

212 Among the 70 putative Fur target sites identified by ChIP-seq analysis, 37 are located in
213 regulatory regions (Fig. 1C-D, Table S4). Most of these sites bind Fur under iron sufficient
214 conditions, although Fur also binds at some sites in at least one of the biological replicates
215 under iron deficient conditions (Table S4). At least twelve of these have good Fur boxes
216 matching to the minimal 7-1-7 consensus sequence (Table S5). Interestingly, Fur binds to the
217 promoter region of *gntR* in an iron-independent manner: Fur occupancy at this site remained
218 about the same level under either iron deficient or sufficient conditions (Table S4).

219 To evaluate the involvement of these putative Fur targets in iron homeostasis, we
220 constructed deletion mutants of the top twelve candidates and carried out assays to test their
221 sensitivity to high levels of iron and dipyridyl (Table S5). None of them showed significant
222 sensitivity to high iron. Five of them showed moderate sensitivity to dipyridyl, including *cspB*,
223 *yhcJ*, *catD*, *narJ*, and *yybN* (Table S5). Transcriptome data suggest that expression of *cspB*, *catD*,
224 and *narJ* might be under regulation of Fur (3). The expression of *catD* is upregulated (3.3)
225 whereas that of *cspB* (0.3) and *narJ* (0.2) is downregulated in a *fur* null mutant compared to the
226 WT strain (Table S5). The regulatory role of Fur in *catD* and *narJ* was further confirmed by
227 mRNA quantification using qPCR (Table S5). Here, the bicistronic operon *catDE* was subject to
228 further investigation to understand its physiological role in iron homeostasis.

229

230 **Fur binds to the regulatory site of *catDE* operon under sufficient iron conditions.**

231 A reproducible ChIP peak was identified in the promoter region of *catDE* operon under
232 sufficient iron conditions. The signal to noise ratio for peak calling is relatively high in both
233 independent replicates (10.1 for Exp.1 and 14.1 for Exp. 2; Fig. 2 and Table S4), and the ChIP
234 DNA enrichment at this site, compared to the input DNA control, is statistically significant (P-
235 value is 3.5×10^{-24} for Exp. 1 and 1.2×10^{-44} for Exp.2; Table S4). The *catDE* operon encodes a
236 putative catechol 2,3-dioxygenase that requires Fe^{2+} as its cofactor (16). CatE showed 2,3-
237 dioxygenase activity *in vitro* and is essential for viability in the presence of catechol (16, 37).

238 We tested the sensitivity of either single (*catD* or *catE*) or double mutant (*catDE*) strains
239 to catechol toxicity using both disk diffusion and bioscreen growth assays. Our results
240 confirmed that they are both involved in catechol detoxification (Fig. S2). Both assays were
241 performed in Belitsky minimal medium because we noticed that the catechol toxicity is
242 significantly diminished in LB medium (Fig. S3), probably due, at least in part, to metal-catechol
243 complexes formed with Fe, Cu, Mn, and other divalent metal ions that are present in LB
244 medium (Fig. S4).

245

246 **Regulation of the *catDE* operon by three regulators**

247 The *catDE* operon is under negative regulation of CatR, a MarR/DUF24 family
248 transcription regulator that senses catechols, and YodB, a regulator of genes important for
249 quinone and diamide detoxification (16). In addition, a Fur box (13 out of 15 bases match to the
250 minimal 7-1-7 consensus sequence; (31)) is located downstream of the transcription start site
251 (Fig 3A), suggesting that Fur may act as a repressor. Indeed, qPCR measurements indicate that

252 expression of *catD* was upregulated ~4-fold in the *fur* null mutant compared to wild-type cells
253 (Fig. 3C), consistent with the previous transcriptome analysis (9).

254 We used electrophoretic mobility shift assays (EMSA) to determine the affinity of Fur for
255 the *catDE* operator site *in vitro*. Surprisingly, unlike the very high affinity ($K_d \sim 0.5\text{-}5.6$ nM)
256 observed for Fur binding to most of its known target sites (3), the affinity of Fur for the *catDE*
257 promoter is quite low ($K_d \sim 0.7$ μM). However, this affinity is comparable to that of either CatR
258 or YodB binding to the same promoter region (16), and all appear to bind rather weakly when
259 tested individually. This suggests that perhaps these three regulators interact with one another
260 and bind to the promoter site cooperatively.

261 To dissect the cooperativity among the three regulators *in vivo*, a genetic study was
262 performed using single, double, and triple deletion mutants of these three regulators and *catD*
263 mRNA levels were quantified under various stress conditions: iron sufficiency, iron limitation,
264 and catechol stress. Consistent with the prior study (16), CatR functions as the major regulator
265 and YodB plays a minor role in regulation of the *catDE* operon (Fig. 3C-D). When only one
266 regulator is present (in the double mutants), YodB repression (in *fur catR* double mutant)
267 resulted in a ~4-fold reduction in mRNA compared to the full derepression observed in the
268 triple mutant (*fur catR yodB*). CatR is the major repressor, and accounts for a ~38-fold reduction
269 of *catD* expression (comparing the *fur yodB* double mutant to the *fur catR yodB* triple mutant).
270 Interestingly, the *catD* mRNA level in *catR yodB* double mutant is comparable to that in the
271 triple mutant, indicating that Fur plays a negligible regulatory role when both CatR and YodB
272 are absent, and Fur binding at this site *in vivo* may require, or facilitated by, the other two
273 regulators.

274

275 **Either CatR or YodB facilitates Fur binding at the promoter site of *catDE***

276 To further explore whether CatR and/or YodB facilitate Fur binding *in vivo*, Fur occupancy
277 at the promote site of *catDE* was evaluated using ChIP-qPCR. No noticeable change of Fur
278 occupancy was observed in the *catR* single mutant compared to wild-type cells, while Fur
279 occupancy increased significantly in *yodB* single mutant (Fig. 4A), indicating that Fur interacts
280 with CatR more efficiently when YodB is absent. This is consistent with the expression data,
281 which showed that *catD* was induced by dipyrindyl in the *catR* single mutant to a level
282 comparable to that observed in the *fur catR* double mutant, whereas it was only partially
283 derepressed by dipyrindyl in the *yodB* single mutant compared to the *fur yodB* double mutant
284 (Fig. 3C). Interestingly, Fur occupancy decreased significantly when both regulators are absent
285 in the *catR yodB* double mutant (Fig. 4A). As expected, neither CatR or YodB affected Fur
286 occupancy at the promoter of *dhbA* (Fig. 4B). These results suggest that CatR, and to a lesser
287 extent YodB, facilitate Fur binding at the promoter region of *catDE*. Similarly, NsrR and ResD
288 have been reported to facilitate Fur binding at a minority of co-regulated sites under anaerobic
289 conditions; at most common sites binding was competitive (15). At the apparently cooperative
290 sites (*ykuN*, *fbpC* and *exlX/yoaJ*), Fur appeared to facilitate binding of NsrR and/or ResD.

291

292 **CatDE is involved in bacillibactin metabolism.**

293 The *B. subtilis* wild type strain (168) and its derivatives does not normally synthesize BB
294 due to a null mutation in the *sfp* gene (*sfp*⁰) encoding the phosphopantetheinyl transferase

295 required for activation of the Dhb NRPS complex. Strains lacking functional Sfp secrete a
296 mixture of 2,3-dihydroxybenzoate (DHBA) and its glycine conjugate (DHBG), collectively known
297 as DHB(G). We use both an *sfp*⁰ strain and an isogenic strain with a corrected *sfp* gene (*sfp*⁺)
298 that produces BB for our iron homeostasis studies.

299 The expression of *catDE* is induced ~3-fold in both *sfp*⁰ and *sfp*⁺ strains upon iron
300 depletion imposed by dipyriddy (Fig. 3 and Fig. 6A-B), suggesting that CatD and/or CatE may be
301 involved in iron homeostasis. To test this idea, dipyriddy sensitivity of single (*catD* and *catE*) and
302 double (*catDE*) mutant strains in both *sfp*⁰ and *sfp*⁺ backgrounds was evaluated using a disk
303 diffusion assay. Indeed, both CatD and CatE play important roles in times of iron limitation since
304 mutants were more strongly growth inhibited in the presence of the iron chelator dipyriddy (Fig.
305 5C-D). We therefore hypothesized that the enzymatic activity of CatDE may be required to
306 detoxify BB-derived catechol compounds produced upon iron limitation. When iron is limited,
307 BB is secreted into the environment to acquire iron and the Fe³⁺-BB complex is imported back
308 into the cell through the FeuABC-YusV system. Iron is released and BB is cleaved into BB
309 monomers (2,3-dihydroxybenzoate-gly-thr), and perhaps further processed into catechol
310 derivatives, which may require CatDE for detoxification.

311 We employed a genetic approach to evaluate the involvement of CatDE in BB
312 metabolism. We used a *fur ymfD* double mutant in which BB is constitutively produced and
313 accumulates intracellularly due to the loss of the YmfD BB exporter. We then asked whether
314 the *catDE* operon is important for growth under these conditions. No growth defects were
315 noticeable in the *fur ymfD catDE* quadruple mutant compared to the *fur ymfD* double mutant in
316 the first 6h, however, dramatic cell lysis was observed in the quadruple mutant afterwards,

317 while the double mutant continued growing (Fig. 6A). We infer that the *catDE* operon is critical
318 for maintaining cell fitness when BB-derived catechol compounds accumulate intracellularly.
319 Indeed, introduction of a *dhbA* null mutation to the quadruple mutant significantly rescued the
320 cell lysis phenotype (Fig. 6A).

321 Once BB is imported back into the cytosol, it is hydrolyzed by the BesA esterase to
322 release the chelated iron and the siderophore is cleaved into three BB monomers. To
323 understand whether the cell lysis defect is due to accumulation of BB or BB monomer, we
324 introduced a *besA* null mutation to the quadruple mutant (*fur ymfD catDE*). In the absence of
325 BesA, cell lysis defect was no longer observed and cells grew almost as well as the *fur ymfD*
326 double mutant (Fig. 6B). It is unknown whether or how BB monomers are further processed.
327 Nevertheless, the BB monomer and perhaps derivative catechol compounds clearly require
328 CatDE for detoxification.

329

330 **Accumulation of intracellular BB-derived catechol induces *catD* expression.**

331 Since intracellular BB-derived catechol compounds can compromise cell fitness, we
332 wished to determine if they might also serve as inducers of the *catDE* operon. To test this, we
333 compared *catD* mRNA levels in the *fur ymfD* double mutant and the *fur* single mutant. Indeed,
334 *catD* expression is increased in the double mutant (defective for BB efflux) compared to the *fur*
335 single mutant. This induction is specifically due to accumulation of intracellular BB-derived
336 catechols since deletion of either *dhbA* or *besA* abolished induction. To understand which
337 regulator is responsible for this induction, we monitored the *catD* mRNA levels in *fur catR* and

338 *fur yodB* double mutants. When both Fur and CatR were absent, induction was no longer
339 evident, suggesting that YodB does not respond to the accumulating catechols. In contrast,
340 when both Fur and YodB were absent, a similar level of induction was observed. These results
341 suggest that intracellular accumulation of BB-derived catechol metabolites can lead to at least
342 partial inactivation of the CatR repressor, thereby leading to induction of the *catDE* operon.
343 Since Fur and CatR bind cooperatively *in vivo*, this system is tuned to respond sensitively to the
344 accumulation of catechol compounds (sensed by CatR) during times of iron starvation (sensed
345 by Fur).

346 **Fur occupancy on the *catDE* operator site**

347 The Fur target genes are derepressed in three sequential waves upon iron depletion (3),
348 which provides insights into the distinct roles of the Fur targets in iron metabolism. To
349 understand the temporal gene expression of *catDE*, we monitored the Fur occupancy on this
350 operator site using a chromosomal FLAG-tagged Fur in both WT and P_{spac} -*frvA*. Using ChIP-qPCR,
351 we found that Fur dissociated rapidly from the DNA binding site and ~50% decrease in Fur
352 occupancy was observed within 3 min upon FrvA induction (Fig. 8). We then compared the Fur
353 occupancy on this site with that on three Fur target sites that are representatives of the three
354 sets of early, middle, and late genes determined previously (3). The results demonstrated that
355 Fur occupancy on the *catDE* operator site followed the same pattern as that on the operator
356 site of the late gene *fsrA* (Fig. 8), suggesting that the *catDE* expression is induced after
357 derepression of BB biosynthesis and BB-mediated uptake systems. We infer that Fur
358 derepression of *catDE* likely occurs soon after the onset of BB synthesis, and this will lead to an
359 initial modest increase in *catDE* expression that will preemptively protect cells against the

360 ensuing import of BB or other catecholate siderophores. In addition, because of the
361 cooperative interaction of Fur and CatR *in vivo*, the loss of Fur repression will also render the
362 CatR repressor more sensitive to accumulating catechols. Together, the loss of Fur and CatR
363 repression will enable the effective detoxification of siderophore-derived catechol compounds.

364

365 **Concluding Remarks**

366 Here we have provided a global overview of potential targets of Fur-mediated gene
367 regulation by mapping of Fur binding sites under iron-replete conditions and after the onset of
368 iron deprivation. Our work confirms the core Fur regulon as defined previously (9), and
369 additionally suggests several new targets deserving of further study. These include potential
370 roles for Fur in regulation of the *S477-ykoP* and *pps* (plipastin synthesis) operons, and in
371 expression of FapR (a regulator of fatty acid synthesis), GidA (a tRNA modifying enzyme), CspB
372 (cold-shock protein) and NarJ (nitrate reductase). Here, we focused our attention on the role of
373 Fur in regulation of *catDE*, encoding a catechol 2,3-dioxygenase.

374 Catechol 2,3-dioxygenase is an exceptionally well-studied enzyme notable for its central
375 role in the biodegradation of a wide variety of aromatic compounds that generate catechol
376 intermediates. Here, we provide a novel example of an endogenously produced intoxicant that
377 relies on CatDE for its degradation (Fig. 9). After import for ferric-bacillibactin into the cytosol,
378 the BesA esterase cleaves the triscatecholate siderophore to release iron yielding three
379 molecules of the BB monomer, 2,3-dihydroxybenzoate-Gly-Thr. In the absence of CatDE, this
380 molecule, or its further degradation products, can be toxic and trigger cell lysis (Fig. 9). The

381 expression of CatDE is under complex control involving three cooperatively functioning
382 repressors. Binding of Fur to the *catDE* regulatory region appears to require cooperative
383 interactions (largely with CatR). Upon the onset of iron deprivation there is an initial modest
384 induction of *catDE* (as inferred from the effect of a *fur* mutation) that will preemptively
385 synthesize CatDE. As catechol compounds accumulate in the cell, due to import and processing
386 of ferric bacillibactin or import of other catecholate xenosiderophores, inactivation of the CatR
387 repressor will lead to full induction. Since Fur and CatR bind cooperatively, once Fur is released
388 the CatR repressor will be more easily inactivated, suggesting that the system will be poised for
389 a rapid response. To our knowledge, this is the first example of an endogenous intoxicant that is
390 catabolized by CatDE. We also present an example of a Fur target that is dependent on the
391 cooperative action of multiple repressor proteins. This is reminiscent of the cooperative
392 interactions documented previously for Fur, NsrR, and ResD reported for cells growing under
393 anaerobic condition (15).

394

395 **Materials and Methods**

396 **Bacterial strains and growth conditions**

397 All strains used in the study are derivatives of *B. subtilis* CU1065 and are listed in [Table S1](#). Cells
398 were grown in LB or Belitsky minimal medium and growth was monitored using a Bioscreen
399 growth analyzer as described in [Text S1](#).

400 **RNA extraction and quantitative PCR (qPCR)**

401 Cells were grown at 37⁰C in LB medium and RNA purified for qPCR analysis as indicated in Text
402 S1 using the indicated primers (Table S2).

403 **Disk diffusion assay**

404 Cells were grown in Belitsky minimal medium and assayed for sensitivity to 10 µl of 1 M
405 catechol or 200 mM dipyriddy as described in Text S1. The data are expressed as the diameter of
406 the inhibition zone (mm).

407 **ChIP-seq, ChiP-qPCR and data analysis**

408 *B. subtilis* cells expressing a C-terminal FLAG-tagged Fur at its native locus and an ectopic copy
409 of *frvA* integrated at *amyE* locus were grown in LB medium amended with 25 µM iron to ensure
410 Fur repression (2). 1 mM IPTG was added to induce expression of FrvA to deplete intracellular
411 iron. ChIP was performed and analyzed by either Illumina-based sequencing (ChIP-seq) or qCR
412 (ChIP-qPCR) as described in detail in Text S1.

413 **Electrophoretic mobility shift assays (EMSA)**

414 Binding of Fur (activated with 1 mM MnC₂) to the *catD* promoter region was monitored using
415 an EMSA assay. The *K_d* value, corresponding to the concentration of Fur that gives rise to 50%
416 half-maximal shifting of the DNA probe, was evaluated and compared to *dhbA* as a positive
417 control.

418

419

420

421

422 References

- 423 1. **Chandrangsu P, Rensing C, Helmann JD.** 2017. Metal homeostasis and resistance in
424 bacteria. *Nat Rev Microbiol* **15**:338-350.
- 425 2. **Andrews SC, Robinson AK, Rodriguez-Quinones F.** 2003. Bacterial iron homeostasis.
426 *FEMS Microbiol Rev* **27**:215-237.
- 427 3. **Pi H, Helmann JD.** 2017. Sequential induction of Fur-regulated genes in response to iron
428 limitation in *Bacillus subtilis*. *Proc Natl Acad Sci U S A* doi:10.1073/pnas.1713008114.
- 429 4. **Pi H, Helmann JD.** 2017. Ferrous iron efflux systems in bacteria. *Metallomics* **9**:840-851.
- 430 5. **Nandal A, Huggins CC, Woodhall MR, McHugh J, Rodriguez-Quinones F, Quail MA,**
431 **Guest JR, Andrews SC.** 2010. Induction of the ferritin gene (*ftnA*) of *Escherichia coli* by
432 Fe(2+)-Fur is mediated by reversal of H-NS silencing and is RyhB independent. *Mol*
433 *Microbiol* **75**:637-657.
- 434 6. **C AS, K RA, Francisco R-Q.** 2003. Bacterial iron homeostasis. *FEMS Microbiology Reviews*
435 **27**:215-237.
- 436 7. **Ollinger J, Song KB, Antelmann H, Hecker M, Helmann JD.** 2006. Role of the Fur regulon
437 in iron transport in *Bacillus subtilis*. *J Bacteriol* **188**:3664-3673.
- 438 8. **Fleischhacker AS, Kiley PJ.** 2011. Iron-containing transcription factors and their roles as
439 sensors. *Curr Opin Chem Biol* **15**:335-341.
- 440 9. **Baichoo N, Wang T, Ye R, Helmann JD.** 2002. Global analysis of the *Bacillus subtilis* Fur
441 regulon and the iron starvation stimulon. *Mol Microbiol* **45**:1613-1629.

- 442 10. **Pi H, Patel SJ, Arguello JM, Helmann JD.** 2016. The *Listeria monocytogenes* Fur-
443 regulated virulence protein FrvA is an Fe(II) efflux P_{1B4}-type ATPase. *Mol Microbiol*
444 **100**:1066-1079.
- 445 11. **Delany I, Rappuoli R, Scarlato V.** 2004. Fur functions as an activator and as a repressor
446 of putative virulence genes in *Neisseria meningitidis*. *Mol Microbiol* **52**:1081-1090.
- 447 12. **Seo SW, Kim D, Latif H, O'Brien EJ, Szubin R, Palsson BO.** 2014. Deciphering Fur
448 transcriptional regulatory network highlights its complex role beyond iron metabolism in
449 *Escherichia coli*. *Nature communications* **5**:4910-4910.
- 450 13. **Davies BW, Bogard RW, Mekalanos JJ.** 2011. Mapping the regulon of *Vibrio cholerae*
451 ferric uptake regulator expands its known network of gene regulation. *Proc Natl Acad*
452 *Sci U S A* **108**:12467-12472.
- 453 14. **Butcher BG, Bronstein PA, Myers CR, Stodghill PV, Bolton JJ, Markel EJ, Filiatrault MJ,**
454 **Swingle B, Gaballa A, Helmann JD, Schneider DJ, Cartinhour SW.** 2011. Characterization
455 of the Fur regulon in *Pseudomonas syringae* pv. tomato DC3000. *J Bacteriol* **193**:4598-
456 4611.
- 457 15. **Chumsakul O, Anantsri DP, Quirke T, Oshima T, Nakamura K, Ishikawa S, Nakano MM.**
458 2017. Genome-Wide Analysis of ResD, NsrR, and Fur Binding in *Bacillus subtilis* during
459 Anaerobic Fermentative Growth by In Vivo Footprinting. *J Bacteriol* **199**.
- 460 16. **Chi BK, Kobayashi K, Albrecht D, Hecker M, Antelmann H.** 2010. The paralogous
461 MarR/DUF24-family repressors YodB and CatR control expression of the catechol
462 dioxygenase CatE in *Bacillus subtilis*. *J Bacteriol* **192**:4571-4581.

- 463 17. **Van Hamme JD, Singh A, Ward OP.** 2003. Recent advances in petroleum microbiology.
464 Microbiol Mol Biol Rev **67**:503-549.
- 465 18. **Mäkelä MR, Marinović M, Nousiainen P, Liwanag AJM, Benoit I, Sipilä J, Hatakka A, de**
466 **Vries RP, Hildén KS.** 2015. Chapter Two - Aromatic Metabolism of Filamentous Fungi in
467 Relation to the Presence of Aromatic Compounds in Plant Biomass, p 63-137. *In*
468 Sariaslani S, Gadd GM (ed), *Advances in Applied Microbiology*, vol 91. Academic Press.
- 469 19. **Seo JS.** 2009. Bacterial Degradation of Aromatic Compounds. **6**:278-309.
- 470 20. **Carmona M, Zamarro MT, Blazquez B, Durante-Rodriguez G, Juarez JF, Valderrama JA,**
471 **Barragan MJ, Garcia JL, Diaz E.** 2009. Anaerobic catabolism of aromatic compounds: a
472 genetic and genomic view. Microbiol Mol Biol Rev **73**:71-133.
- 473 21. **Nina S, B. ZAJ, L. ERI.** 2001. Chemical properties of catechols and their molecular modes
474 of toxic action in cells, from microorganisms to mammals. *Environmental Microbiology*
475 **3**:81-91.
- 476 22. **Raymond KN, Dertz EA, Kim SS.** 2003. Enterobactin: an archetype for microbial iron
477 transport. *Proc Natl Acad Sci U S A* **100**:3584-3588.
- 478 23. **May JJ, Wendrich TM, Marahiel MA.** 2001. The *dhb* operon of *Bacillus subtilis* encodes
479 the biosynthetic template for the catecholic siderophore 2,3-dihydroxybenzoate-
480 glycine-threonine trimeric ester bacillibactin. *J Biol Chem* **276**:7209-7217.
- 481 24. **Miethke M, Schmidt S, Marahiel MA.** 2008. The major facilitator superfamily-type
482 transporter YmfE and the multidrug-efflux activator Mta mediate bacillibactin secretion
483 in *Bacillus subtilis*. *J Bacteriol* **190**:5143-5152.

- 484 25. **Miethke M, Klotz O, Linne U, May JJ, Beckering CL, Marahiel MA.** 2006. Ferri-
485 bacillibactin uptake and hydrolysis in *Bacillus subtilis*. *Mol Microbiol* **61**:1413-1427.
- 486 26. **Gamba P, Jonker MJ, Hamoen LW.** 2015. A Novel Feedback Loop That Controls Bimodal
487 Expression of Genetic Competence. *PLoS Genet* **11**:e1005047.
- 488 27. **Albanesi D, de Mendoza D.** 2016. FapR: From Control of Membrane Lipid Homeostasis
489 to a Biotechnological Tool. *Front Mol Biosci* **3**:64.
- 490 28. **Schujman GE, Paoletti L, Grossman AD, de Mendoza D.** 2003. FapR, a bacterial
491 transcription factor involved in global regulation of membrane lipid biosynthesis. *Dev*
492 *Cell* **4**:663-672.
- 493 29. **Comella N, Grossman AD.** 2005. Conservation of genes and processes controlled by the
494 quorum response in bacteria: characterization of genes controlled by the quorum-
495 sensing transcription factor ComA in *Bacillus subtilis*. *Mol Microbiol* **57**:1159-1174.
- 496 30. **Guan G, Pinochet-Barros A, Gaballa A, Patel SJ, Arguello JM, Helmann JD.** 2015. PfeT, a
497 P_{1B4} -type ATPase, effluxes ferrous iron and protects *Bacillus subtilis* against iron
498 intoxication. *Mol Microbiol* **98**:787-803.
- 499 31. **Baichoo N, Helmann JD.** 2002. Recognition of DNA by Fur: a reinterpretation of the Fur
500 box consensus sequence. *J Bacteriol* **184**:5826-5832.
- 501 32. **Tsuge K, Ano T, Hirai M, Nakamura Y, Shoda M.** 1999. The genes *degQ*, *pps*, and *lpa-8*
502 (*sfp*) are responsible for conversion of *Bacillus subtilis* 168 to plipastatin production.
503 *Antimicrob Agents Chemother* **43**:2183-2192.
- 504 33. **Nicolas P, Mader U, Dervyn E, Rochat T, Leduc A, Pigeonneau N, Bidnenko E,**
505 **Marchadier E, Hoebeke M, Aymerich S, Becher D, Bisicchia P, Botella E, Delumeau O,**

- 506 **Doherty G, Denham EL, Fogg MJ, Fromion V, Goelzer A, Hansen A, Hartig E, Harwood**
507 **CR, Homuth G, Jarmer H, Jules M, Klipp E, Le Chat L, Lecointe F, Lewis P, Liebermeister**
508 **W, March A, Mars RA, Nannapaneni P, Noone D, Pohl S, Rinn B, Rugheimer F, Sappa**
509 **PK, Samson F, Schaffer M, Schwikowski B, Steil L, Stulke J, Wiegert T, Devine KM,**
510 **Wilkinson AJ, van Diji JM, Hecker M, Volker U, Bessieres P, et al. 2012. Condition-**
511 dependent transcriptome reveals high-level regulatory architecture in *Bacillus subtilis*.
512 Science **335**:1103-1106.
- 513 34. **Vivek R, Gunaseelan D, Ramya K, Ramkrishna S, Mahitosh M. 2012. Time-dependent**
514 dosing of Fe²⁺ for improved lipopeptide production by marine *Bacillus megaterium*.
515 Journal of Chemical Technology & Biotechnology **87**:1661-1669.
- 516 35. **Wei YH, Wang LF, Chang JS. 2004. Optimizing iron supplement strategies for enhanced**
517 surfactin production with *Bacillus subtilis*. Biotechnol Prog **20**:979-983.
- 518 36. **Mulligan CN, Yong RN, Gibbs BF, James S, Bennett HPJ. 1999. Metal Removal from**
519 Contaminated Soil and Sediments by the Biosurfactant Surfactin. Environmental Science
520 & Technology **33**:3812-3820.
- 521 37. **Nguyen VD, Wolf C, Mader U, Lalk M, Langer P, Lindequist U, Hecker M, Antelmann H.**
522 2007. Transcriptome and proteome analyses in response to 2-methylhydroquinone and
523 6-brom-2-vinyl-chroman-4-on reveal different degradation systems involved in the
524 catabolism of aromatic compounds in *Bacillus subtilis*. Proteomics **7**:1391-1408.

525

526 **Figure legends**

527 **Fig. 1. An overview of Fur-binding profiles across the *B. subtilis* genome under varied iron**
528 **conditions.**

529 A. ChIP-seq data of *B. subtilis* Fur-dependent binding under iron sufficient and deficient
530 conditions. Two biological replicates were included for each growth condition (Exp. 1 and Exp.
531 2). Reads are in blue with maximum set at 1500 for all the ChIP peaks. The total reads for each
532 sample are included on the left side. S/N denotes signal to noise ratio for peak calling as shown
533 in brown.

534 B. Most of ChIP peaks (22 out of 27) identified under iron deficient conditions overlap with
535 those detected under iron sufficient conditions. The majority of peaks (61 out of 94) are located
536 in regulatory regions.

537 C. Most of the known Fur binding sites from the literature (24 out of 27) are identified by ChIP-
538 seq with three exceptions. Among all the new identified Fur binding sites, 33 sites are located in
539 intragenic regions while 37 sites are located in regulatory regions.

540 D. Distribution of ChIP peaks relevant to S/N ratio. The highest S/N ratio of each ChIP peak
541 among all four samples was used for this analysis.

542

543 **Fig. 2. Fur binds to the promoter region of *catDE* operon under iron replete conditions.**

544 A zoom-in example of Fur binding at the *catDE* operate site identified by ChIP-seq. Two
545 biological replicates were included as Exp.1 and Exp.2 for each condition. A single peak was
546 annotated at this region for both replicates under iron sufficient conditions. The peak length
547 was 328 bp for Exp. 1 and 355 bp for Exp. 2. No peaks were annotated at this region for either
548 replicate under iron deficient conditions. S/N denotes signal to noise ratio for peak calling.

549

550 **Fig. 3. Regulation of the *catDE* operon by three transcription factors**

551 A. The promoter sequence of the *catDE* operon: -10, -35, and the transcriptional start site (+1)
552 are highlighted in blue; the two CatR boxes are indicated by orange arrows; the YodB box is
553 indicated by light blue arrow; the Fur box is underlined.

554 B. Electrophoretic mobility shift assay (EMSA) was carried out to determine Fur-DNA binding
555 affinity to the promoter region of the *catDE* operon. Experiments were repeated three times
556 and a representative image is shown.

557 C. The *catD* mRNA levels were compared among different strains grown in LB medium without
558 or with 100 μ M dipyridyl using qPCR.

559 D. The *catD* mRNA levels were compared among different strains grown in Belitsky minimal
560 medium without or with 2 mM catechol using qPCR. The 23S rRNA gene was used as an internal
561 control for both C and D.

562

563 **Fig. 4. Either CatR or YodB facilitates Fur binding at the promoter site of *catDE*.**

564 Fur occupancy was evaluated by chromatin immunoprecipitation (ChIP) using anti-FLAG
565 antibodies. Coimmunoprecipitated DNA was quantified by qPCR. DNA enrichment was
566 calculated based on the input DNA (1% of total DNA used for each ChIP experiment). The Data
567 are presented as the fold enrichment of Fur occupancy at the promoter sites of *catDE* (A) and
568 *dhbA* (B) (mean \pm SD; n = 3). Significant differences between wild type and mutant strains are

569 indicated: **P < 0.01. No significant DNA enrichment was observed for *gyrA* that serves as a
570 negative control.

571

572 **Fig. 5. *catDE* is induced upon iron depletion and plays an important role in iron homeostasis.**

573 (A,B) Expression of *catD* was monitored in wild-type cells (A, *sfp*⁰; B, *sfp*⁺) grown in LB medium
574 before (0 min) and after treatment of 100 μM dipyriddy. Significant difference between treated
575 and untreated groups is indicated as ** P < 0.01.

576 (C,D) Dipyriddy sensitivity of WT, single (*catD* and *catE*), and double (*catDE*) mutant strains in
577 both *sfp*⁰ (C) and *sfp*⁺ (D) backgrounds was evaluated using a disk diffusion assay. The data are
578 expressed as the diameter (mean ± SEM; n = 3) of the inhibition zone (mm). Significant
579 differences between wild type and mutant strains are indicated: * P < 0.05 and ** P < 0.01.

580

581 **Fig. 6. CatDE is involved in BB metabolism.**

582 (A, B) Representative growth curves are shown for strains that constitutively produce BB (*fur*
583 mutation) and accumulate BB intracellularly (due to loss of the BB exporter YmfD). To check
584 whether CatDE is required for BB metabolism growth of wild type (*sfp*⁺) and its derived mutant
585 strains was monitored in LB medium for 25 h. Experiments were performed three times with
586 three biological replicates each time.

587

588 **Fig. 7. Accumulation of intracellular BB-derived catechol induces *catD* expression.**

589 The mRNA expression levels of *catD* was evaluated in WT (*sfp*⁺) and its derived mutants grown
590 in LB medium to an OD₆₀₀ of ~0.4. The 23S rRNA was used as an internal control. Significant
591 differences are indicated as *P < 0.05 and **P<0.01. NS denotes not significant.

592 **Fig. 8. Fur occupancy on different operator sites.**

593 Fur occupancy was evaluated by CHIP-qPCR. DNA enrichment was calculated based on the input
594 DNA (1% of total DNA used for each CHIP experiment). Fur occupancy at different sites was set
595 as 100% at zero time-point. Dates are presented as the relative percentage (%) of occupancy at
596 different time points after 1 mM IPTG induction of FrvA (mean ± SEM; n = 3). No significant DNA
597 enrichment was observed for *gyrA* that is used as a nonspecific negative control.

598

599 **Fig. 9. Correlation between BB metabolism and catechol detoxification**

600 The endogenous siderophore BB is synthesized by an NRPS (non-ribosomal peptide synthetase)
601 assembly system (DhbACEBF) (23) and secreted by a major facilitator superfamily transporter
602 YmfD, which is under regulation of the transcriptional activator Mta, a MerR family regulator of
603 multidrug-efflux transporter system (24). BB chelates iron with very high affinity and the
604 resulting ferric-BB complex is then imported back into the cytosol through the FeuABC-YusV
605 system and hydrolyzed by the BesA esterase to release iron (25), which yields three BB-
606 monomers (2,3-dihydroxybenzoate-Gly-Thr). It is still unknown whether or how the BB
607 monomer is further processed. Nonetheless, it is clear that the BB monomer and perhaps BB-
608 derived catechol compounds require CatDE for detoxification during metabolism.

609

610

611

612

613

614

615 **Text S1. Materials and Methods**

616 **Table S1. Strains and plasmids used in this study**

617 **Table S2. Primer oligonucleotides**

618 **Table S3. Known Fur targets associated with CHIP-peaks.**

619 **Table S4. Putative Fur-regulated genes associated with CHIP-peaks**

620 **Table S5. Putative Fur target genes evaluated in this study**

621

622 **Fig. S1. putative Fur binding sites specifically under iron deplete conditions.**

623 Putative apo-Fur binding sites identified in the intragenic regions of: (A) *spo0B*, (B) *flhB*, (C) *xynP*, and (D)

624 *ylpC* (also known as *fapR*). Two biological replicates were included as Exp.1 and Exp.2 for each condition.

625 S/N denotes signal to noise ratio for peak calling.

626

627 **Fig. S2. CatDE is critical for catechol degradation.**

628 Sensitivity of the *sfp*⁰ (A) and *sfp*⁺ strains (B) to catechol was evaluated in Belitsky minimal medium

629 using a disk diffusion assay. 10 µl of 1 M catechol was applied to each disk. The data are expressed as the

630 diameter (mean ± SEM; n = 3) of the inhibition zone (mm). Significant differences between wild type and

631 mutant strains are indicated: **P < 0.01.

632 Representative growth curves in Belitsky minimal medium with *sfp*⁰ (C) and *sfp*⁺ strains (D). 2mM

633 catechol was used for both sets of experiments.

634

635 **Fig. S3. Catechol toxicity is diminished in LB medium**

636 Representative growth curves of WT and *catD* null mutant strains grown in LB medium without or with
637 addition of 8mM catechol.

638

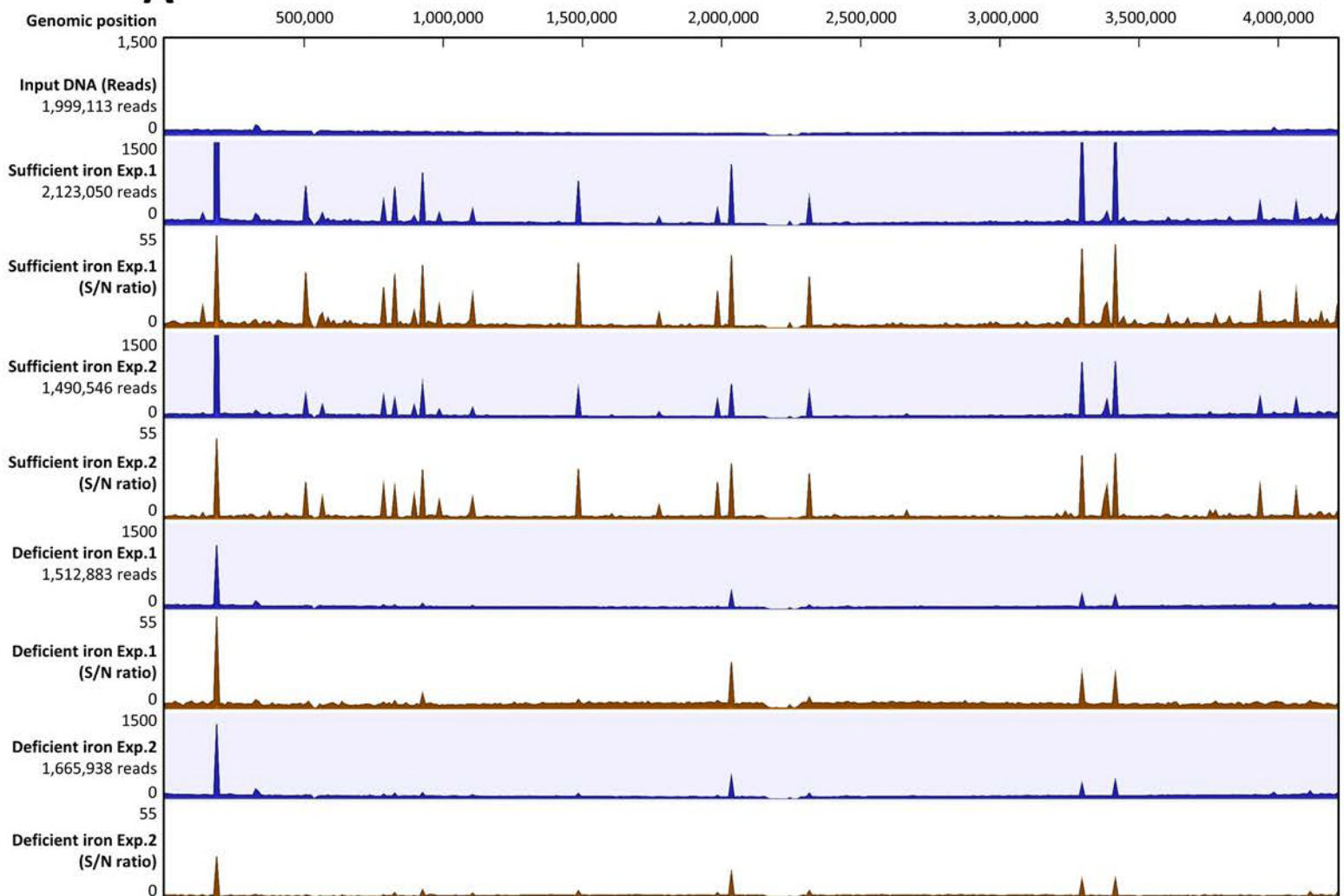
639 **Fig. S4. Metal-catechol complexes alleviates catechol intoxication**

640 Representative growth curves of *sfp⁺ catD* mutant cells grown in Belitsky minimal medium without or
641 with addition of 2mM catechol. To evaluate the effects of metal-catechol complexes on catechol
642 intoxication, different concentrations of metal salts were tested: (A) FeSO₄, (B) CuSO₄, (C) MnCl₂, and (D)
643 ZnCl₂.

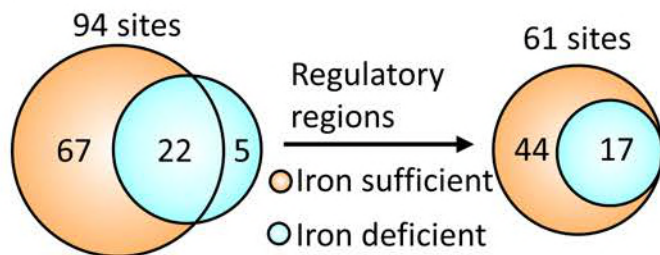
644

645

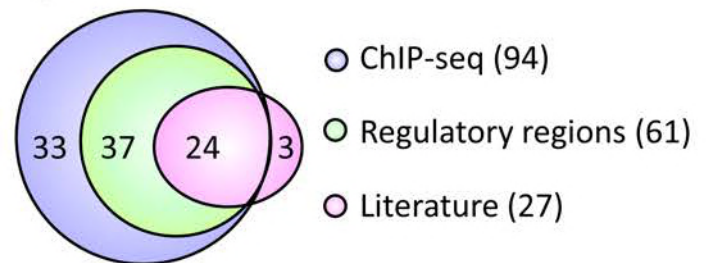
A



B



C



D

